GIS-Based Modelling of Soil Erosion Risk Categories County Antrim, Northern Ireland

Zeinab Smillie

University of Stirling

The paper is a non-peer-reviewed preprint submitted to EarthArXiv

Abstract

Soil erosion is one of the major global concerns. Such a process can occur naturally, at different rates. However, under extreme conditions, soil erosion can accelerate and present a risk to ecosystems, loss of food supply (loss of agricultural lands), and lead to episodic landslides.

The present study employs Geographic Information Systems and functions to predict possible risks connected to soil erosion based on the knowledge of topographical data, average rainfall, soil types and landcover data. The study combines different risk factors to produce different models.

Different risk maps were produced to better visualise the spatial distribution of soil erosion risk categories. The influence of ground slope, rainfall and soil texture was evident via the models. The addition of the landcover factor hugely modified the risk categories distribution. It is clear that some habitats, such as wetlands and forests, can increase soil stability and reduce soil erosion risk.

Introduction

Soil erosion is one of the significant soil threats to many ecosystems and human survival. Soil erosion is defined as "the accelerated removal of topsoil from the land surface through water, wind and tillage" (FAO, 2022). Hence, Soil erosion is a key global concern as it can result in land degradation, loss of agricultural land and reduction in food production.

The Earth's ground is subject to different natural processes, including adverse effects of climate conditions, including wind, rainfall and ice action (Mitasova et al., 2013). In addition, human activities can cause negative influences on natural systems, including soil ecosystems and soil stability.

Soil erosion is a natural process and is part of "weathering", where surface soil particles are transported from one place to another to form new sediments or soils in other areas. However, unsustainable human activities put additional pressure on the environment. Adverse human activities such as intensive agriculture, modification of drainage, soil extraction and dredging, deforestation, overgrazing and excessive or inappropriate land use can change the soil erosion patterns and are known to accelerate the erosion processes and the loss of many ecosystems (ClimateXChange, 2018; FAO, 2022). The amount of soil that can be deposited through natural processes may take thousands or millions of years and can be destroyed and wasted under unsustainable human action within decades (Chapman, 2017).

Understanding the combined influences of natural factors presents a challenge in processing and interpreting the data. However, the advancement of geographic information systems (GIS) and remote sensing (RS) techniques helped to revolutionise the ways that various data can be integrated into different models or scenarios to predict various national hazards (Coppock, 1995;

Tarolli and Cavalli, 2013). Examples are fluvial erosion (Finlayson and Montgomery, 2003; Lazzari, 2020; Strager et al., 2010), and landslides (Mersha and Meten, 2020).

For example, combining topographic data with various data such as landcover, climatic, and hydraulic makes the GIS technique an excellent candidate for watershed analysis and coastal erosion analysis. e.g. (Boardman et al., 2009; El Jazouli et al., 2017; Teshome et al., 2021)

The technique is fast developing, and the accessibility of data, methods and programming scripts means more extensive engagement of users, application of the techniques, sharing of the experience and improvement of the method.

Soil erosion, in particular, is a high risk connected to natural factors such as rainfall-runoff. This effect of rainfall can be magnified where steep grounds exist. Soil texture also plays a fundamental role. Coarser friable soils such as sands and sandy loam soils are more prone to erosion compared to more cohesive finer-grained (clayey) soils.

Other factors may influence soil erosion. For example, organic matter may exist in mucus filaments that bind soil particles together and increase the resistance to erosion by natural elements (Chapman, 2017). The loss of organic matter due to excessive human activities such as vegetation removal can increase the risk of deterioration of agricultural lands, especially when combined with inadequate soil structure and intense rainfall (ClimateXChange, 2018).

The study area is located in the northern part of Northern Ireland and is part of County Antrim (Fig. 1).

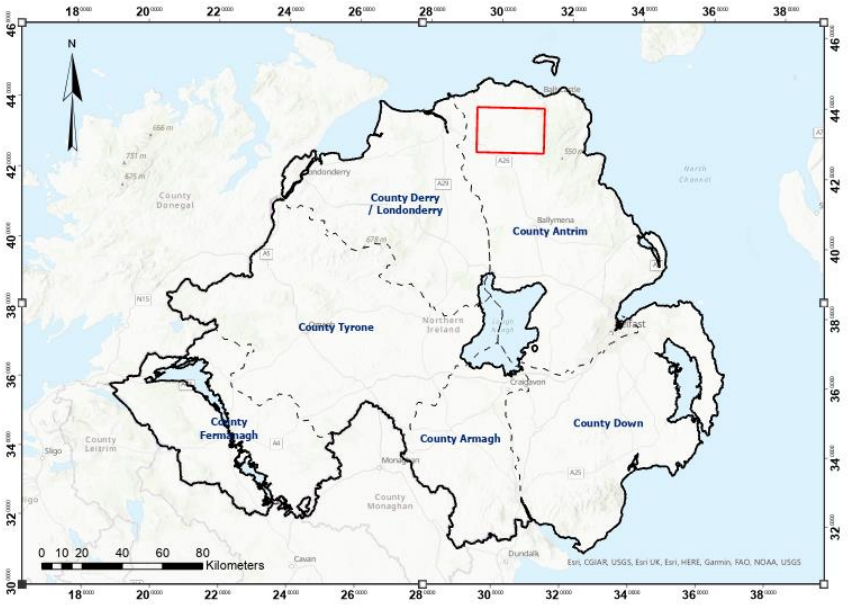

Fig. 1: Location of the study area (red square) within Northern Ireland.

The area was selected for the present study due to its importance to agriculture, as most of the site is covered by agriculture and natural lands (Fig. 2). However, the area also receives moderate to high rainfall (Fig. 3), which increases runoff and potential soil erosion.

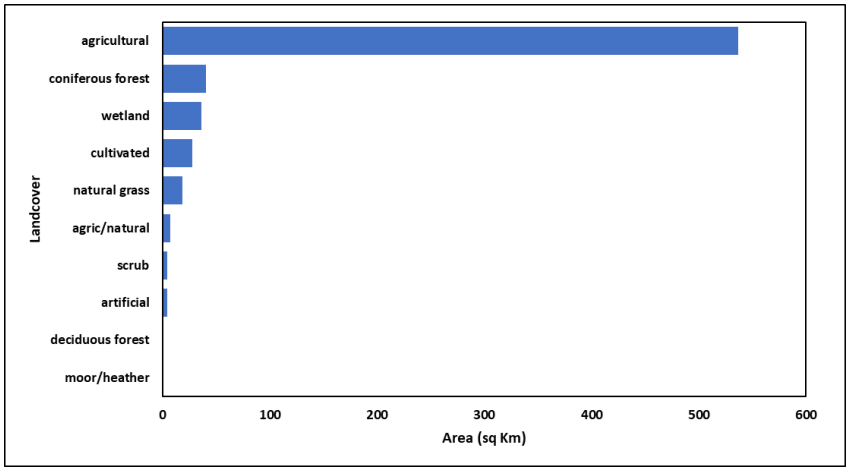

Fig. 2: Distribution of landcover in the study area.

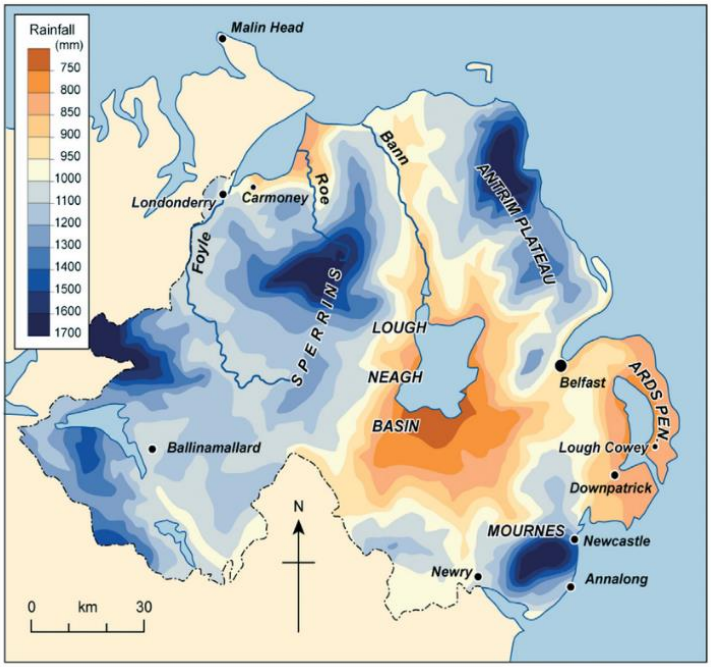

Fig. 3: Average annual precipitation (in mm) in Northern Ireland, 1961–1990 (after (Betts, 2002))

The present study is structured upon the knowledge of the soil textures, topography (esp. ground slope) and the amount of rainfall. These are assumed to be the main factors influencing soil erosion. Additional information regarding the land cover is used to assess the final soil erosion risk categories.

The main goal of the present study is to develop and apply a model of the risk of soil erosion. This will be achieved through achieving the following objectives.

1) Understanding the topography of the area in respect of elevation and slope aspects.
2) Interpret the combined effect of different natural factors (ground slope, soil texture and the amount of rainfall)
3) Combine these factors to present different models predicting soil erosion patterns across the study area.
4) Assess the effect of landcover on the soil erosion categories in the area.

Methodology

Raw data include topographic data (raster), rainfall (shapefile) and soil map (shapefile). A list of these data and their providers is provided in table 1. These data were used to derive GIS layers with detailed or classified categories for the analyses required (Table 2 and Fig. 4).

Table 1: List of the data used in this study.

Data	Dataset	Type	Source
Rainfall	Rainfall data (in mm)	Shapefile (point data)	(MetOffice, 2022)
Slope	Contour data 1:50,000 scale	Shapefile (line data)	(OSNI, 2015)
soil texture	Soil data 1:10,000 scale	Shapefile (polygon data)	(AFBI, 2015)
land cover	Landcover data 1:100,000 scale	Shapefile (polygon data)	(Copernicus, n.d.)

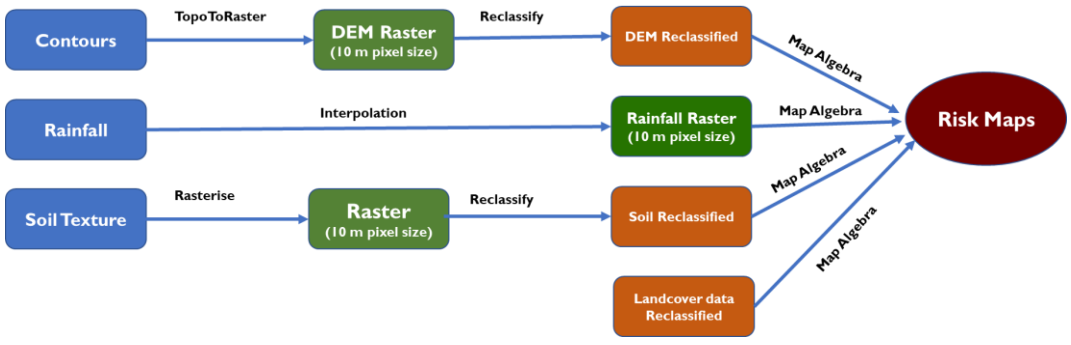

Fig. 4: Flowchart showing key steps in transforming the data into reclassified raster to fit the raster map algebra calculations and producing soil erosion risk maps.

Table 2: List of derived layers during the preparation of this study.

Data	Dataset	Method	Output	Pixel Size (m)
Rainfall	Rainfall	Interpolation	Raster	10
Slope (derived from contours)	Slope_risk	Raster reclassify	Raster	10
Soil	Soil	Polygon to Raster	Raster	10
Soil	Soil_risk	Raster reclassify	Raster	10
land cover	land cover	Polygon to Raster	Raster	10
land cover	IC_risk	Raster reclassify	Raster	10

A digital elevation model (DEM) was created using the TopoToRaster function. First, the raster pixel size was set at 10 m. This value is less than the minimum spatial contour spacing (Fig. 5); hence raster at this resolution would keep most of the details inherited from the raw data. All the data were then converted into a raster with the same pixel size (10m).

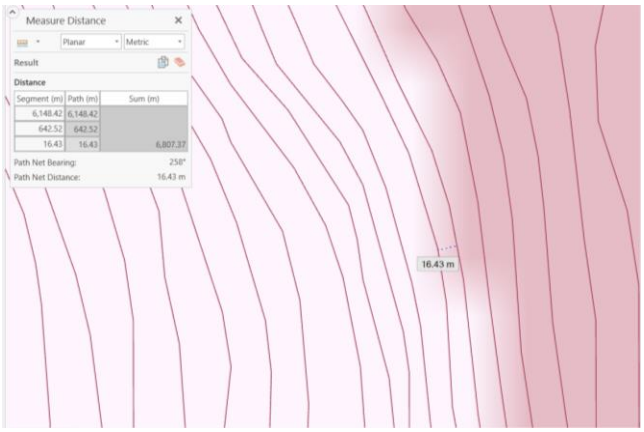

Fig. 5: Minimum value of the spatial spacing of the contours in the study area is shown as 16 m.

Slope data were then derived from the DEM raster layer, using "Percent_Rise". A copy of the slope layer was then created and reclassified (0 – 4) to match the slope risk categories. Details of soil types and parent rocks in the area are provided in Appendix 1.

Soils (attribute Layer 2) in the area were classified into three categories, classification on the mainframe used by ESDAC (2022):

1. Risk category 1: mainly coarse friable soils such as sand, loamy sand, sandy loam, sandy silt loam, silt loam.
2. Risk category 2: medium-grained soils such as silty clay loam.
3. Risk category 3: Any other soils, usually more cohesive fine-grained soils.

Some soil types are not classified (not allocated a class) due to either their artificial or mixed nature, including:

1. DIST = Disturbed land
2. URB = Urban areas & other built-up areas

Heavy rainfall can accelerate soil erosion and causes flooding and mass wasting, including landslides (Piacentini et al., 2018). The study area suffers high rainfall, above 900 ml. The threshold of increased risk due to rainfall is >= 800 mm, putting all parts of the area under high rainfall risk. Hence no rainfall data classification was attempted. However, the rainfall data was a prominent part of the analysis.

Rainfall data were integrated into a raster using the interpolation method from the Geostatistical Wizard in ArcGIS Pro. Various interpolations methods were examined, with multiple parameters such as power, maximum and minimum number of neighbours.

The interpolation model predicts the value and location of additional points where data are missing to provide semicontinuous or continuous data. Cross-validation is used to evaluate the trend, and prediction model, i.e. compares the actual (measured) and missing (predicted) values. Root-Mean-Square (RMS) indicates how the predicted model (interpolation) deviates from the original data trend. The smaller the RMS, the more accurate the model. The best method was the local polynomial interpolation (ESRI, 2022), as it showed the lowest RMS of 12.44 (Fig. 6 a).

Other methods tested included the Inverse distance weighted (IDW), which is best used when there are dense data enough to show local variations (Watson and Philip, 1985). However, the RMS when IDW is applied was considerably low (16.03) compared to radial basis functions (43.57), see Fig. 6 b & c.

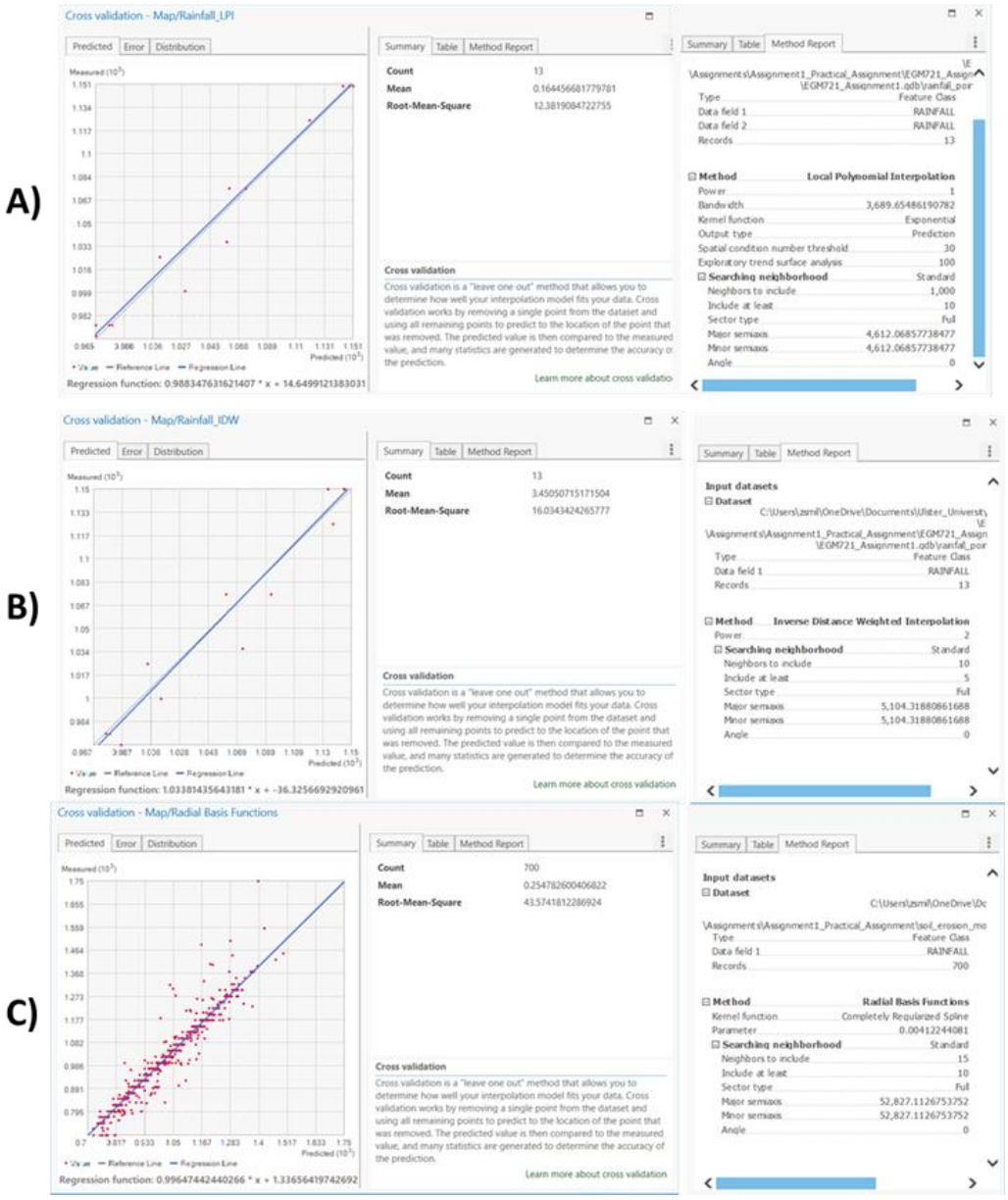

Fig. 6: Comparison of the interpolation methods Local Polynomial Interpolation, IDW and radial basis functions. The cross-validation report of the IDW (interpolation method) is the lowest, hence used to convert the rainfall discrete (point) data into continuous data (raster).

Both elevation and soil data were then classified according to their risk categories (Table 3). Each newly produced copy of the data layers was then named using meaningful names. Various iterations of raster calculations were then applied to create different layers representing a specific level of soil erosion risk.

Table 3: Risk categories using soil and slope degrees. The average annual rainfall in the area is > 800 mm. Hence, rainfall data is not included in the table.

Soil Textures (Risk categories 1-3)	**Slopes > 7 ° (Steep)**	**Slopes 3 ° - 7 ° (Moderate)**	**Slopes 2 ° - 3 ° (Gentle)**	**Slope < 2 ° (Level ground)**
Risk category 1	Very high	High	Moderate	Slight
Risk category 2	High	Moderate	Lower	Slight
Risk category 3	Lower	Slight	Slight	Slight

Different Booleans were employed to add conditional criteria or sum pixel values from the raster layers. In addition, scripts provided in Tables 4 and 5 were used to produce other risk categories.

The output rasters were binary, with the "0" (zero) value indicating pixel values that do not match the criteria in the syntax, while "1" shows the pixels with values that match the syntax.

Table 4: Scripts used to create raster layers showing various risk categories.

Risk Category	Code	Output Layer
Model 1 (Soil risk category 1: sand, loamy sand, sandy loam, sandy silt loam, silt loam)		
Very High Risk	(("Soil_risk" == 1) & ("Slope_risk" == 1) & ("Rainfall" >= 800))	M1_VH_Risk
High Risk	(("Soil_risk" == 1) & ("Slope_risk" == 2) & ("Rainfall" >= 800))	M1_H_Risk
Medium Risk	(("Soil_risk" == 1) & ("Slope_risk" == 3) & ("Rainfall" >= 800))	M1_M_Risk
Slight Risk	(("Soil_risk" == 1) & ("Slope_risk" == 4) & ("Rainfall" >= 800))	M1_S_Risk
Model2 (Soil risk category 2: silty clay loam)		
High Risk	(("Soil_risk" == 2) & ("Slope_risk" == 1) & ("Rainfall" >= 800))	M2_H_Risk
Medium Risk	(("Soil_risk" == 2) & ("Slope_risk" == 2) & ("Rainfall" >= 800))	M2_M_Risk
Lower Risk	(("Soil_risk" == 2) & ("Slope_risk" == 3) & ("Rainfall" >= 800))	M2_L_Risk
Slight Risk	(("Soil_risk" == 2) & ("Slope_risk" == 4) & ("Rainfall" >= 800))	M2_S_Risk
Model 3: (Soil risk category 3: other mineral soils)		
Medium Risk	(("Soil_risk" == 3) & ("Slope_risk" == 1) & ("Rainfall" >= 800))	M3_M_Risk
Slight Risk	(("Soil_risk" == 3) & ("Slope_risk" == 2) & ("Rainfall" >= 800))	M3_S_Risk
Slight Risk	(("Soil_risk" == 3) & ("Slope_risk" == 3) & ("Rainfall" >= 800))	M3_S_Risk
Slight Risk	(("Soil_risk" == 3) & ("Slope_risk" == 4) & ("Rainfall" >= 800))	M3_S_Risk

Table 5: Scripts used to create overall risk category maps.

Risk Category	Script
Very High	"M1_VH_Risk"
High	(("M1_VH_Risk" == 1) | ("M1_H_Risk" == 1) | ("M2_H_Risk" == 1))
Moderate	(("M1_H_Risk" == 1) | ("M1_M_Risk" == 1) | ("M2_H_Risk" == 1) | ("M2_M_Risk" == 1))
Lower	(("M1_M_Risk" == 1) | ("M2_L_Risk" == 1) | ("M3_L_Risk" == 1))
Slight	(("M1_S_Risk" == 1) | ("M2_S_Risk" == 1) | ("M3_S1_Risk" == 1) | ("M3_S2_Risk" == 1) | ("M3_S3_Risk" == 1))

The risk layers were then reclassified with unique values each, to be used in the final step of integration to produce one map showing the distribution of different risk categories, taking into account the three factors: soil composition, ground slope, and rainfall. The final syntax to integrate all the risk layers together was:

(("Reclass_VH") + ("Reclass_H") + ("Reclass_M") + ("Reclass_L") + ("Reclass_S"))

Landcover data were processed to produce a 10 m pixel size raster. These data were then classified into five different risk categories, where 0 values were assigned to landcover that has no risk class most of the area, class 1 (slight risk) corresponds to agricultural land, agricultural/natural lands, and coniferous forest, primarily found in low-moderate elevated grounds, class 2 (low risk) corresponds to wetland and scrubs, class 3 (moderate) matches natural grass, cultivated, and heathlands and finally class 4 represents a high risk, associated with agricultural land.

This method of reclassification and Boolean was repeated by adding the landcover data to the risk layers.

Results and Discussion

The study area is dominated by low lands and gentle slopes (Figs 7), which may assume that soils are at low risk of erosion. However, the eastern part of the area is characterised by hilly grounds with high elevations (> 500 m above sea level) and steep slopes (~ 47 °). This particular part of the area experience high rainfalls (up to 1149 mm). However, all the study area receives high precipitation, above 900 mm (Fig. 8).

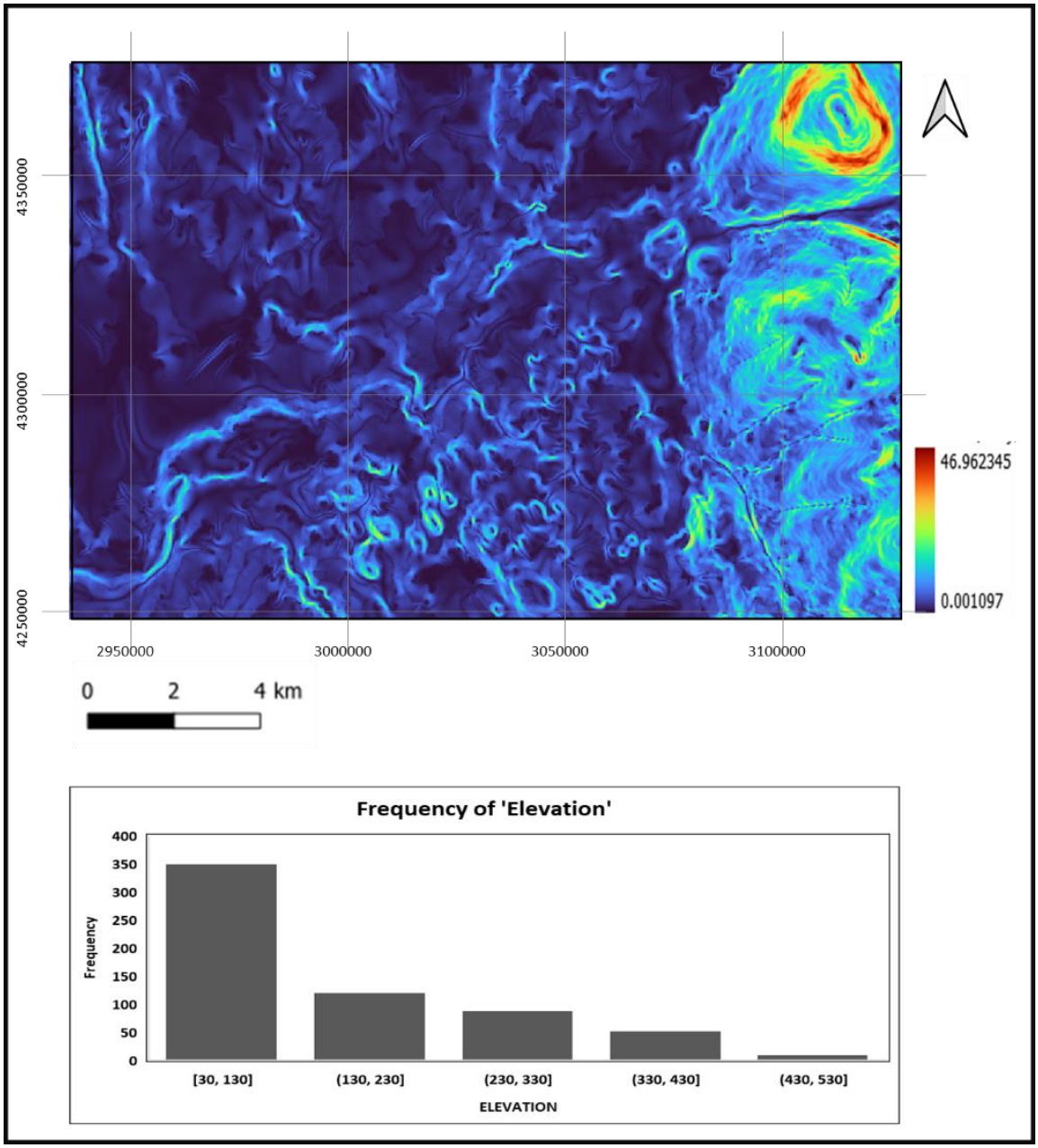

Fig. 7: Distribution of slope angles (top) and elevation in m (bottom) in the study area.

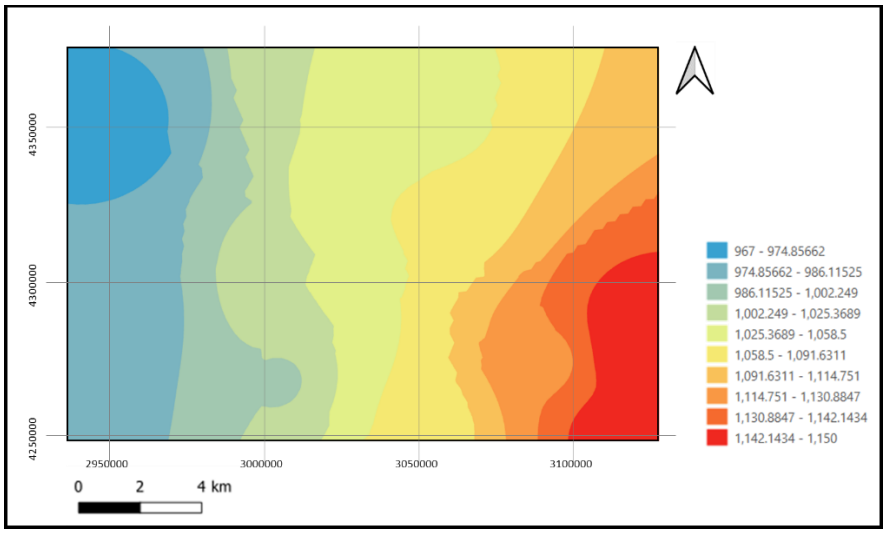

Fig. 8: Rainfall data (interpolated). Classes displayed represent geometrical intervals.

The combinations of topography and rainfall aspects pose a considerable risk of soil erosion in these eastern parts of the area. However, the soil and landcover nature may equally influence the soil erosion processes.

Figures 9 & 10 and Appendix I show the distribution of soils in the study area. These data show that the dominant bedrocks are of basaltic composition. These rocks are basic in composition and more vulnerable to weathering than granitic rocks under the effect of natural forces. The predominant soil types in the area are gleys, humic Gley, and peatlands. Peatlands (maroon colour on Fig. 10) are known as excellent carbon sinks. The disturbance of these lands would release the carbon into the atmosphere and increase the greenhouse gases in the atmosphere.

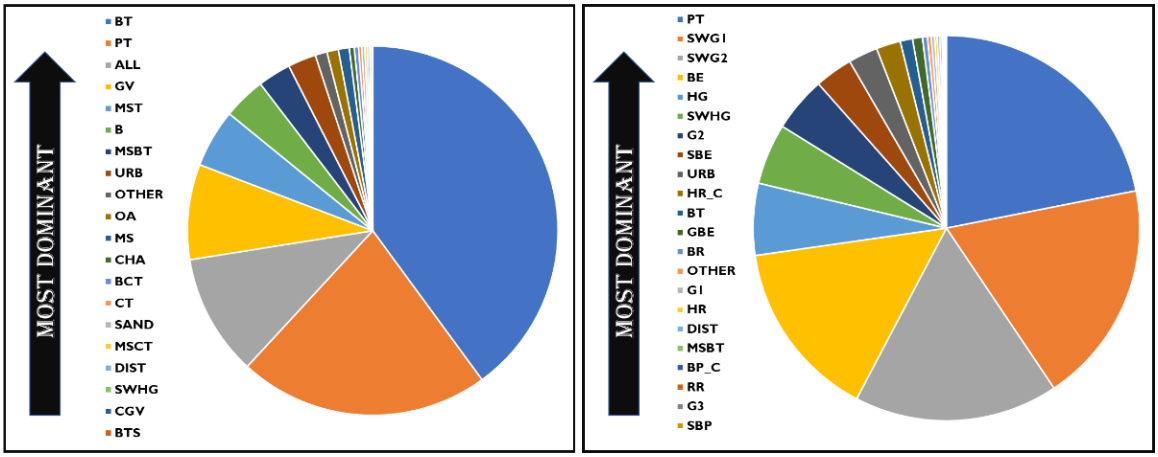

Fig. 9: Distribution of soil (left) and soil parent rocks (right) in the area. Codes are explained in Appendix

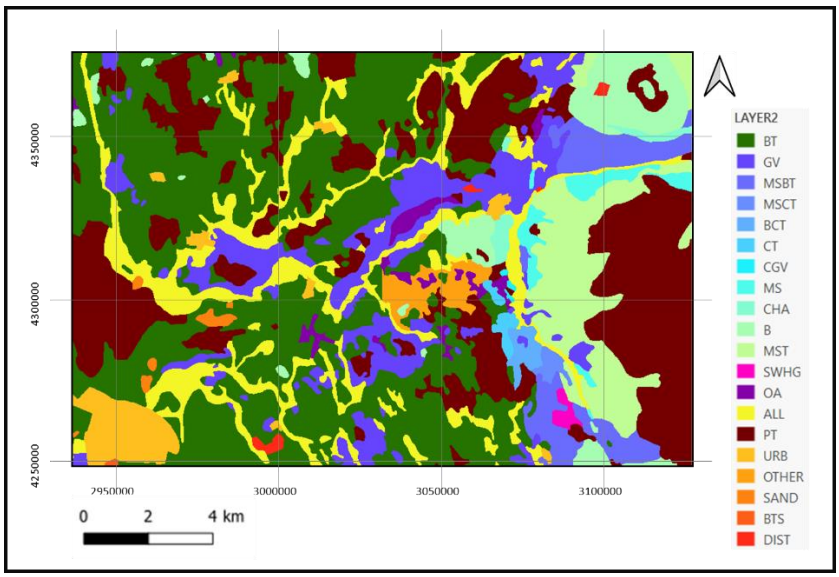

Fig. 10: Soil types distribution in the study area. The codes are explained in Appendix I.

The area is covered mainly by agricultural lands (Fig. 11). It is noted that wetland and coniferous forests are common on highlands to the east, while farming lands cover most of the low and moderate elevations.

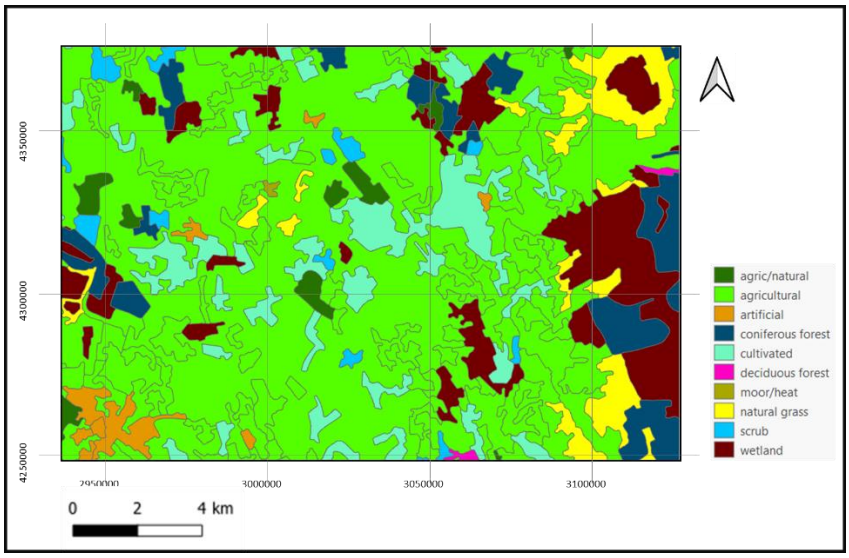

Fig. 11: Landcover map of the study area

The risk classes adopted in the present study indicate the capacity of potential erosion risk to the soil by combining the factors of the slope, soil types and rainfall. Fig. 12 shows the matrix of soil erosion as a result of combining both soil composition risk factors and ground slope. As the area suffers high rainfall (>900 mm), this is well above the threshold of high rainfall risk. Hence, this is not shown in the matrix. However, it was included in the syntax used to produce the mini-maps of risk distribution in Fig 11. It is well noted that ground slope significantly influences soil

erosion. This is observed in the top-left mini-map in Fig. 12, where a very high soil erosion risk is associated with steep grounds. On the other hand, moderate soil erosion is estimated in some moderate to steep grounds in both the highlands to the east and lowlands to the west.

Where the slope becomes gentler, the soil texture effect becomes apparent. For example, the highland peats and/or where the soil is waterlogged are associated with a "lower" risk. In contrast, the low lands covered by natural/agricultural soils show a slight risk category.

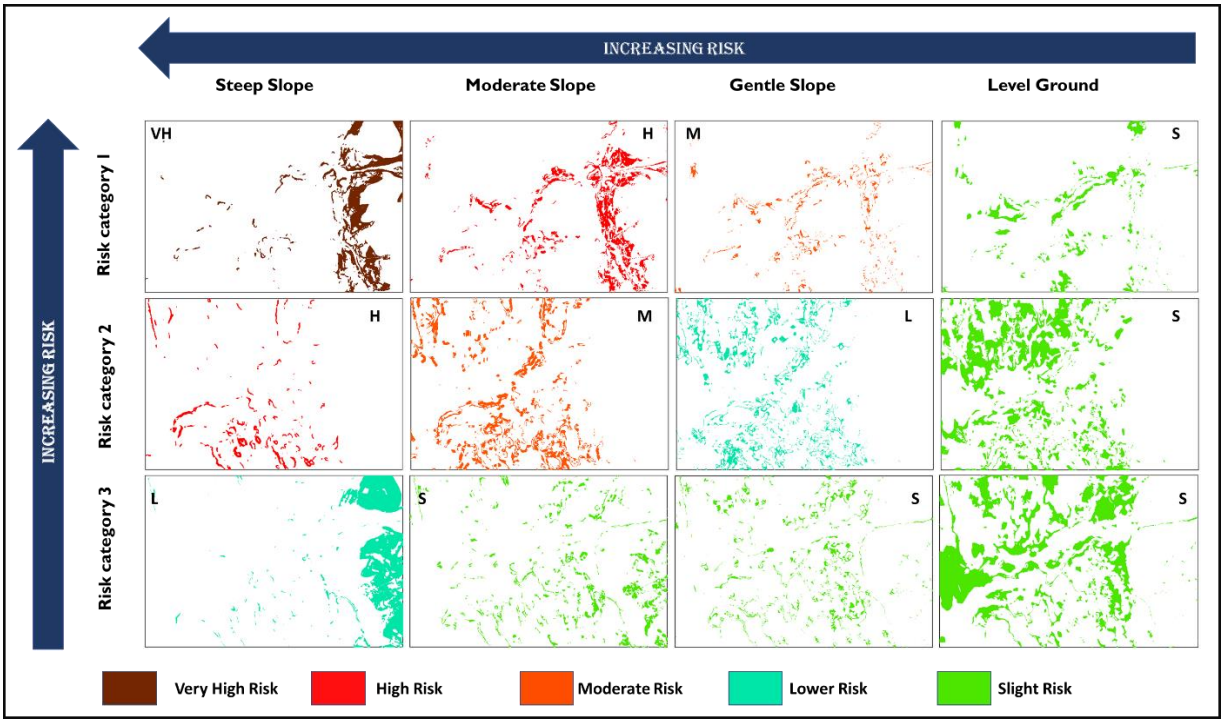

Fig. 12: Soil erosion risk in relation to the soil risk categories (left) and ground slope risk (top). The colours indicate different soil erosion risks. The white areas indicate no risk considering each case's input soil and slope factors.

The results of integrating all the risk rasters are shown in Fig. 13. At this stage, a raster was produced for each risk category.

In general, the results show that the eastern part of the area is more subject to soil erosion, considering the excessive rainfall and the steep grounds in these specific parts. However, the soils in some of these parts are covered with wetlands and forest lands. Some of these forests help the preservation of the soil from erosion. This is clear at the top of the hills. However, the edges of the hills are predicted to suffer more erosion and mass wasting.

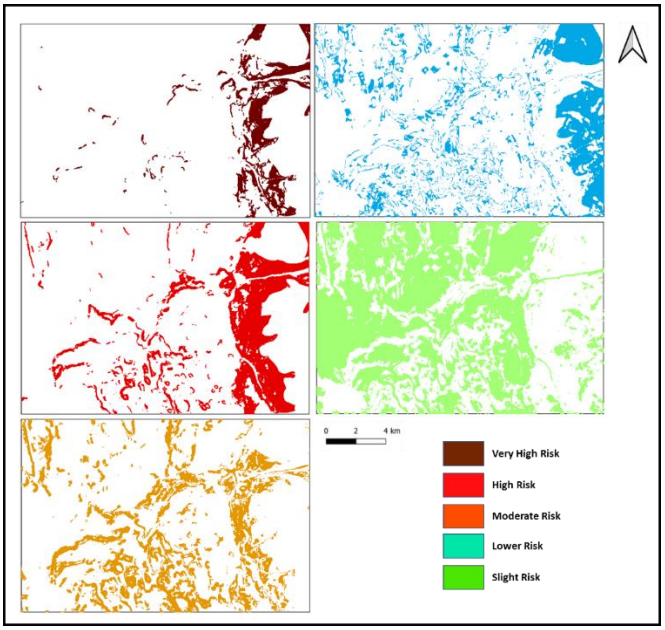

Fig. 13: Overall soil erosion categories, combining the soil composition, slope degrees and rainfall.

A final step was to combine all the five risk categories into one map. Figure 14 shows detailed risk maps. Moderate soil erosion risk categories are associated with steep to moderate grounds in all parts of the study area. However, they are more concentrated to the east. Despite their moderate slope, some places seem to be protected from soil erosion (dark green). These are artificial or urban landscapes. It is also clear that the top of the hills is at "lower" risk while steep grounds are at moderate to very high risk.

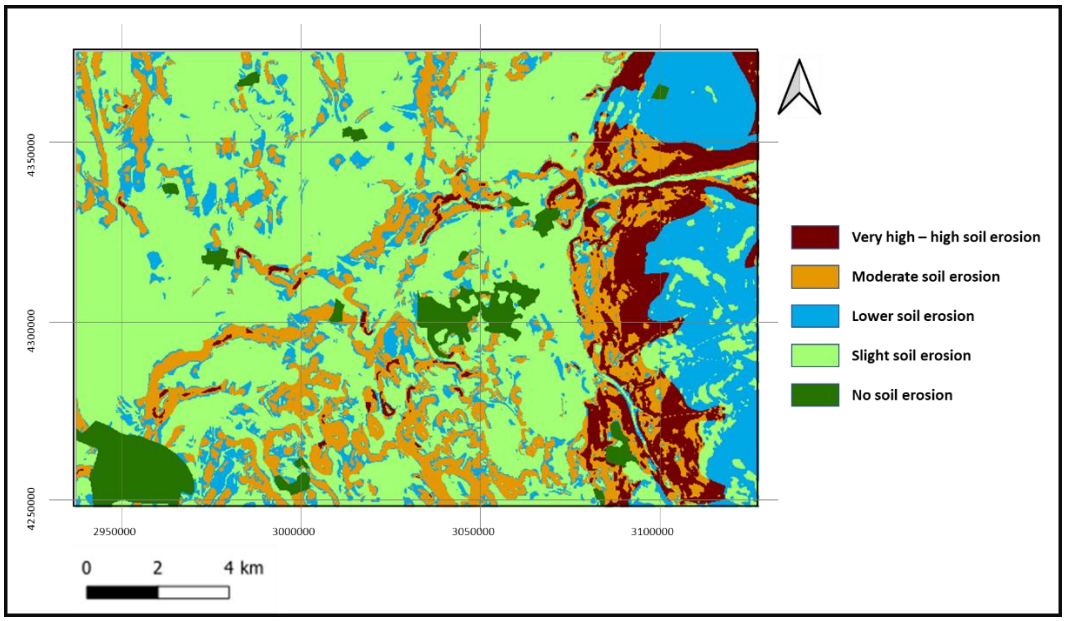

Figure 14: Detailed soil risk erosion map of the study area.

These risk classes are revised by including the landcover data, as indicated in Table 6 and Fig. 15. It is clear that the addition of landcover can generally reduce (category-wise and spatial distribution) the soil erosion risk despite the fact that the calculated risk from the first three forces (soil type, slope and rainfall) could indicate very high or high risk. However, it may increase the risk in some places, e.g. bare soil with no vegetation cover is more likely to be eroded than areas covered by vegetation.

Table 6: Risk categories based on soil texture, slope gradient, rainfall and landcover.

Land cover risk category	**Erosion risk categories derived from Table 3**				
	Very high	**High**	**Moderate**	**Lower**	**Slight**
4	Very high	High	High	Moderate	Moderate
3	High	Moderate	Moderate	Lower	Lower
2	Moderate	Moderate	Lower	Lower	Slight
1	Moderate	Lower	lower	Slight	Slight
0	None	None	None	None	None

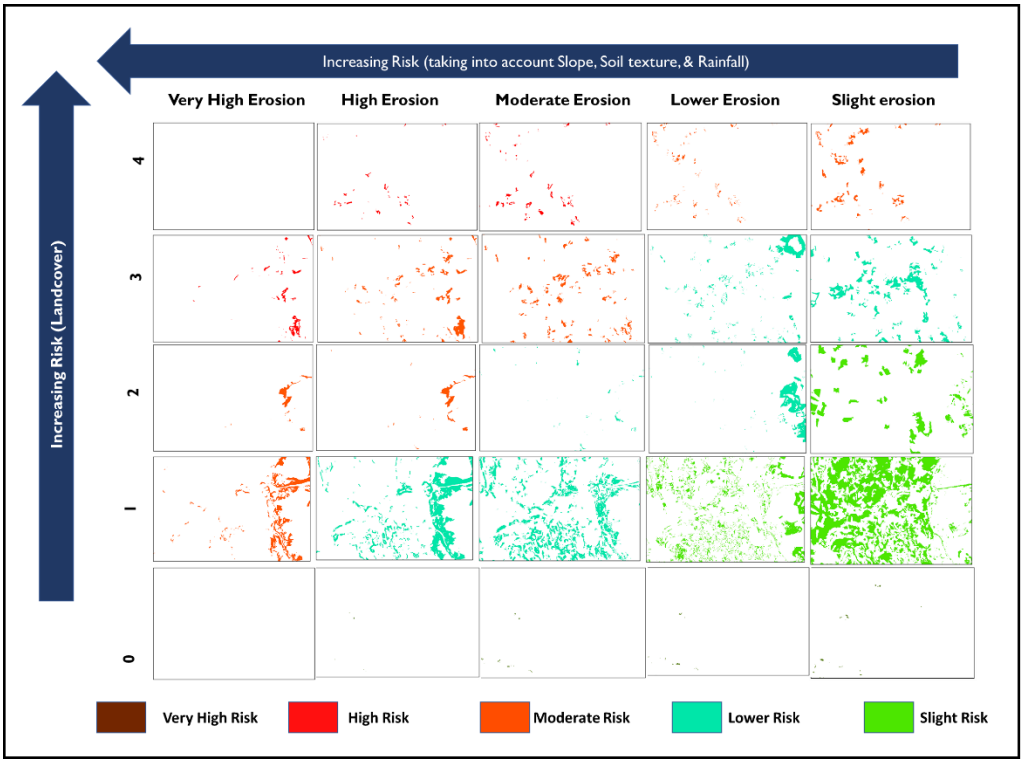

Fig. 15: Effect of landcover upon soil erosion risk categories.

Conclusions and recommendations

The study presents a visual presentation and modelling of the contribution of various natural factors influencing soil erosion in the study area of Northern Ireland. The study employed different data types, including discrete data (rainfall) and polygon data. Using various GIS functions such as interpolation, geostatistical layers, and raster calculation, it was possible to transform discrete data into continuous data (through prediction/modelling) and combine effects of natural factors to build various models predicting different soil erosion scenarios based on risk factors.

The results demonstrated the influence of natural forces on soil erosion risk. It also produced prediction models when combining different factors. It is noted that slope, soil types, rainfall, and landcover influence soil erosion. Topography (especially slope gradients) influence the erosion models that can be primarily modified when considering soil texture and landcover.

It is recommended to integrate more information such as hydrological data (including fluvial systems) to produce more accurate prediction models.

References

AFBI, 2015. Soil maps and soil survey. https://www.afbini.gov.uk/articles/soil-maps-and-soil-survey

Betts, N., 2002. Climate Change in Northern Ireland, in: Smyth, A., Montgomery, W.I., Favis-Mortlock, D., Allen, S. (Eds.), Implications of Climate Change for Northern Ireland, Informing Strategy Development. Stationery Office, pp. 26–42.

Boardman, J., Shepheard, M.L., Walker, E., Foster, I.D.L., 2009. Soil erosion and risk-assessment for on- and off-farm impacts: A test case using the Midhurst area, West Sussex, UK. J. Environ. Manage. 90, 2578–2588. https://doi.org/10.1016/j.jenvman.2009.01.018

Chapman, P.J., 2017. Soils, in: Holden, J. (Ed.), An Introduction to Physical Geography and the Environment. Pearson, Harlow, England Munich.

ClimateXChange, 2018. Soil erosion and compaction in Scottish soils: adapting to a changing climate.

Copernicus, 2012. CORINE Land Cover. https://land.copernicus.eu/pan-european/corine-land-cover

Coppock, J.T., 1995. Gis and Natural Hazards: An overview from a Gis Perspective, in: Carrara, A., Guzzetti, F. (Eds.), Geographical Information Systems in Assessing Natural Hazards, Advances in Natural and Technological Hazards Research. Springer Netherlands, Dordrecht, pp. 21–34. https://doi.org/10.1007/978-94-015-8404-3_2

El Jazouli, A., Barakat, A., Ghafiri, A., El Moutaki, S., Ettaqy, A., Khellouk, R., 2017. Soil erosion modeled with USLE, GIS, and remote sensing: a case study of Ikkour watershed in Middle Atlas (Morocco). Geosci. Lett. 4, 25. https://doi.org/10.1186/s40562-017-0091-6

ESDAC, 2022. Soil Erosion Risk Assessment in Europe [WWW Document]. Eur. SOIL DATA Cent. URL https://esdac.jrc.ec.europa.eu/ESDB_Archive/serae/GRIMM/erosion/inra/europe/analysis/maps_and_listings/web_erosion/presentation.html

ESRI, 2022. Understanding interpolation analysis—ArcGIS Pro | Documentation [WWW Document]. URL https://pro.arcgis.com/en/pro-app/2.8/tool-reference/spatial-analyst/understanding-interpolation-analysis.htm

FAO, 2022. Soil erosion | Global Soil Partnership | Food and Agriculture Organization of the United Nations [WWW Document]. Food Agric. Organ. U. N. URL https://www.fao.org/global-soil-partnership/areas-of-work/soil-erosion/en/

Finlayson, D.P., Montgomery, D.R., 2003. Modeling large-scale fluvial erosion in geographic information systems. Geomorphology 53, 147–164. https://doi.org/10.1016/S0169-555X(02)00351-3

Lazzari, M., 2020. GIS Application in Fluvial Geomorphology and Landscape Changes. Water 12, 3481. https://doi.org/10.3390/w12123481

Mersha, T., Meten, M., 2020. GIS-based landslide susceptibility mapping and assessment using bivariate statistical methods in Simada area, northwestern Ethiopia. Geoenvironmental Disasters 7, 20. https://doi.org/10.1186/s40677-020-00155-x

MetOffice, 2022. Rainfall Sampling Points. https://www.metoffice.gov.uk/research/climate/maps-and-data/data/index

Mitasova, H., Barton, M., Ullah, I., Hofierka, J., Harmon, R.S., 2013. 3.9 GIS-Based Soil Erosion Modeling, in: Treatise on Geomorphology. Elsevier, pp. 228–258. https://doi.org/10.1016/B978-0-12-374739-6.00052-X

OSNI, 2015. Contour data 1:50,000 scale. https://www.nidirect.gov.uk/articles/150000-vector

Piacentini, T., Galli, A., Marsala, V., Miccadei, E., 2018. Analysis of Soil Erosion Induced by Heavy Rainfall: A Case Study from the NE Abruzzo Hills Area in Central Italy. Water 10, 1314. https://doi.org/10.3390/w10101314

Strager, M.P., Fletcher, J.J., Strager, J.M., Yuill, C.B., Eli, R.N., Todd Petty, J., Lamont, S.J., 2010. Watershed analysis with GIS: The watershed characterisation and modeling system software application. Comput. Geosci. 36, 970–976. https://doi.org/10.1016/j.cageo.2010.01.003

Tarolli, P., Cavalli, M., 2013. Geographic Information Systems (GIS) and Natural Hazards, in: Bobrowsky, P.T. (Ed.), Encyclopedia of Natural Hazards, Encyclopedia of Earth Sciences Series. Springer Netherlands, Dordrecht, pp. 378–385. https://doi.org/10.1007/978-1-4020-4399-4_152

Teshome, A., Halefom, A., Teshome, M., Ahmad, I., Taddele, Y., Dananto, M., Demisse, S., Szucs, P., 2021. Soil erosion modelling using GIS and revised universal soil loss equation approach: a case study of Guna-Tana landscape, Northern Ethiopia. Model. Earth Syst. Environ. 7, 125–134. https://doi.org/10.1007/s40808-020-00864-0

Watson, D.F., Philip, G.M., 1985. A Refinement of Inverse Distance Weighted Interpolation. Geoprocessing 2, 315–327.

Appendix I

Table I-1 Distribution of various soil types in the area.

Code	Area (sq Km)	Soil Types
PT	67.24	All types of peat >50cm0%
SWG1	57.49	Surface Water Gley 10%
SWG2	52.49	Surface Water Gley 20%
BE	46.20	Brown Earth >40cm to C Horizon0%
HG	18.53	Stagno-Humic Gley0%
SWHG	15.68	Surface Water Humic Gley0%
G2	14.18	Ground Water Gley 20%
SBE	9.77	Shallow Brown Earths(40-60cm deep)0%
URB	7.56	Urban areas & other built-up areas0%
HR_C	6.24	Humic ranker complex0%
BT	3.18	Basalt CL till0%
GBE	2.53	Gleyed brown earth0%
BR	1.28	Brown Rankers(inc BE & BP rankers)0%
OTHER	0.98	scanning level0%
G1	0.86	Ground Water Gley 10%
HR	0.67	Humic ranker0%
DIST	0.63	Disturbed land0%
MSBT	0.56	Mixed Mica-Schist & basalt till0%
BP_C	0.44	Brown Podzolic(with Bs horizon)0%
RR	0.30	Raw Skeletal0%
G3	0.21	Ground Water Gley 30%
SBP	0.18	Shallow brown podzol0%

Table I-2: Land areas (in square kilometres) underlined by each parent rock type, with the associated soil types.

Row Labels	Area (sq Km)	Soil	Bedrock
BT	122.75	Surface Water Gley	Basalt till
PT	67.24	Brown Earth and Surface Water Gley	Chalk/gravel
ALL	32.68	Surface Water Humic Gley	Mixed Mica-Schist & basalt till
GV	25.61	Disturbed land	
MST	15.65	Brown Earth and Surface Water Gley	Mica schist and chalk till
B	11.42	Brown Earth	Sand
MSBT	8.88	Brown Earth	Chalky Till
URB	7.56	Brown Earth and Surface Water Gley	Basalt and chalk till
OTHER	3.18	Shallow Brown Earths and Brown Rankers	Chalk
OA	3.07	Shallow Brown Earths, Shallow Brown Podzol, Brown Rankers, Brown Podzolic and Raw Skeletal	Mica-Schist
MS	2.92	Ground Water Gley	Organic/Mineral Alluvium
CHA	1.34	Basalt CL till	
BCT	1.15	Urban/Built areas	
CT	0.84	Brown Earth and Surface Water Gley	Mixed Mica-Schist & basalt till0%
SAND	0.82	Shallow Brown Earths, Shallow Brown Podzol, Brown Rankers, Brown Podzolic and Raw Skeletal	Basalt rock
MSCT	0.68	Surface Water Gley/Humic Gley	Mica-Schist till
DIST	0.63	Brown Earth	Gravel
SWHG	0.56	Ground Water Gley, Stagno-Humic Gley, and Brown Earth	Alluvial
CGV	0.15	Peat	
BTS	0.07	Surface Water Gley, Surface Water Humic Gley and Gleyed brown earth	Basalt till stone free0%